

Original Article

Bioinformatic profiling of prognostic microenvironment-related genes in Wilms tumors

Xiao Liang, Yuan Hu, Tao Yi

Key Laboratory of Obstetrics & Gynecologic and Pediatric Diseases and Birth Defects of Ministry of Education, Development and Related Diseases of Women and Children Key Laboratory of Sichuan Province, West China Second Hospital, Sichuan University, Chengdu 610041, Sichuan Province, China

Received February 24, 2021; Accepted September 6, 2021; Epub December 15, 2021; Published December 30, 2021

Abstract: Wilms tumor (WT), is one of the most common types of extracranial solid tumors found in early childhood, and it needs positive attention worldwide. The tumor microenvironment (TME) serves as a key role in the aggressiveness of tumors and has been investigated in many kinds of tumors, primarily in adult-onset cancers. However, the TME is not well studied in childhood tumors, especially in Wilms tumors. In the present study, we performed a systematic investigation of the genetic factors associated with the Wilms tumor microenvironment with the help of bioinformatics and TARGET database (Therapeutically Applicable Research to Generate Effective Treatments, <https://ocg.cancer.gov/programs/target>). The stromal and immune scores of patients were calculated with an “ESTIMATE” algorithm and the TME-related differentially expressed genes (TME-related DEGs) were detected with the R package “limma”. Then their functional analysis was further revealed by “ClusterProfiler”. The direct/indirect correlations between TME-related DEGs were assessed with STRING and the protein-protein interaction (PPI) network was then reconstructed by Cytoscape. The DEGs in the top two clusters selected by Molecular Complex Detection (MCODE) were taken as hub genes. Survival analysis of all the DEGs was studied and the prognostic immune-related biomarkers for Wilms tumors were detected. In this study, stromal scores were found to be closely associated with the overall survival of Wilms tumor patients. TME-related DEGs and hub genes were suggested to participate in the migration and function of immune cells. What’s more, 11 of them including GSDMA, TRIM55, SPARCL1, EPHY2, LRRCC2, LAPTM5, PTGFR, APOD, IGF1, CEBPD and SFRP2, were significantly associated with overall survival of patients. In brief, our study arrived at a more comprehensive understanding of the tumor microenvironment and provided more data for decoding the complicated microenvironment in Wilms tumors by identified several prognostic biomarkers.

Keywords: Tumor microenvironment, Wilms tumor, data mining, TARGET database

Introduction

Wilms tumor (WT) is one of the most frequent extracranial solid tumors seen in early childhood (<15 years age) [1]. Wilms tumors originate from kidney precursor cells that spread to other vital organs (such as lungs, liver, bone, brain or nearby lymph nodes) and this diagnosis leads to a poor prognosis [2]. With the improvement of medical care, the prognosis of Wilms tumors has been improved [3]. However, as a malignant tumor mainly occurring in young children, its occurrence and development requires more attention and further study. In order to investigate better pathogenesis and determine better treatment methods for Wilms tumor patients, many studies have been performed and have provided new perspectives for

biologists with regard to Wilms tumor treatment [4, 5]. Genetic alterations of tumor cells including somatic, germline mutations and intrinsic gene dysregulation have been reported to dictate the initiation, progression, and evolution of Wilms tumors [6-10].

On the other hand, the tumor microenvironment which refers to all of the physiological and biochemical elements at the tumor site beside tumor cells, consists of many different non-cancerous cells including stromal cells and immune cells [11]. The tumor microenvironment has profound impacts on tumor progression and metastasis [12] and is increasingly recognized as a non-negligible obstacle to cancer theranostics and therapeutics [13]. Thus, further study of the tumor microenvironment may

help for effective theranostics and therapeutics of cancer. However, these investigations were primarily performed in adult-onset cancers and little is known about childhood tumors, especially Wilms tumors.

Upregulation of the immune associated factors such as vascular endothelial growth factor (VEGF) and hypoxia-inducible factor 1 (HIF-1) in the tumor microenvironment have been observed to recruit immune cells in Wilms tumors [14]. However, these studies were restricted to only one or two immune markers of Wilms tumors. In this study we provide a comprehensive view of the microenvironment in Wilms tumors with bioinformatics analysis.

Stromal and immune cells were proposed as major non-cancer components at the tumor site and are valuable for cancer theranostics and therapeutics, thus algorithm such as “ESTIMATE” designed by Yoshihara was developed to predict tumor purity [15]. With this algorithm, stromal and immune scores can be calculated via analyzing the expression of specific gene signatures of immune/stromal cells and predict the infiltration of immune/stromal cells. ESTIMATE algorithm has been quickly applied to bioinformatics analysis of prostate cancer [16], breast cancer [17], glioblastoma [18] and colon cancer [19] and has revealed a list of prognosis immune-associated genes but it has not been applied to the study of Wilms tumors.

In the current work, the gene expression data obtained from TARGET database was analyzed with ESTIMATE algorithm. We extracted a list of tumor microenvironment related differentially expressed genes (TME-related DEGs) and hub genes for the first time which were significantly associated with migration and function of immune cells in the Wilms tumor microenvironment that need further study.

Materials and methods

Data acquisition and processing

A total of 121 Wilms tumor patients with complete clinical information and RNA expression data were enrolled in the study. All the RNA sequencing data and the corresponding clinical data for Wilms tumor patients were obtained from Therapeutically Applicable Research to Generate Effective Treatments (TARGET)

(<https://ocg.cancer.gov/programs/target>). Stromal and immune scores were calculated by ESTIMATE, an algorithm providing scores for the level of stromal cells present and the infiltration level of immune cells in tumor tissues [15].

Survival analysis

Taking the median immune/stromal score as the cutoff value, Wilms tumor patients were classified into either a high immune/stromal score group or low immune/stromal score group. A univariate Cox model was used to illustrate the correlation between immune/stromal score and patients' overall survival (OS).

Wilms tumor patients were classified into a high or low expression group by taking the median expression value of specific TME-related DEGs as the cutoff value. Then specific TME-related DEGs associated survival analysis between these two groups were evaluated by Kaplan-Meier survival curve and log-rank test analysis. The TME-related DEGs which were significantly associated with patients' overall survival (OS) were screened out with $P < 0.05$ as the threshold for statistical significance.

Identification of differentially expressed genes (DEGs) and TME-related DEGs

According to the ESTIMATE results, all Wilms tumor patients were divided into high/low groups based on their stromal or immune score. Then the expression of genes was identified with R package “limma”. $|\log_2 FC| > 1$ (FC = fold change) and false discovery rate (FDR) < 0.05 were set as the cutoffs to identify differentially expressed genes (DEGs). Heatmaps were generated with R package “pheatmap”.

TME-related DEGs was defined as intersection genes which were upregulated or downregulated in both Stromal-related genes and Immune-related genes.

Functional enrichment analysis

Gene Ontology (GO) functional enrichment analysis and Kyoto Encyclopedia of Genes and Genomes (KEGG) pathway enrichment analysis of TME-related DEGs were conducted using the R package “clusterProfiler” [20]. $P < 0.05$ was set as the statistical significance threshold cri-

Prognostic microenvironment related gene mining in a Wilms tumor

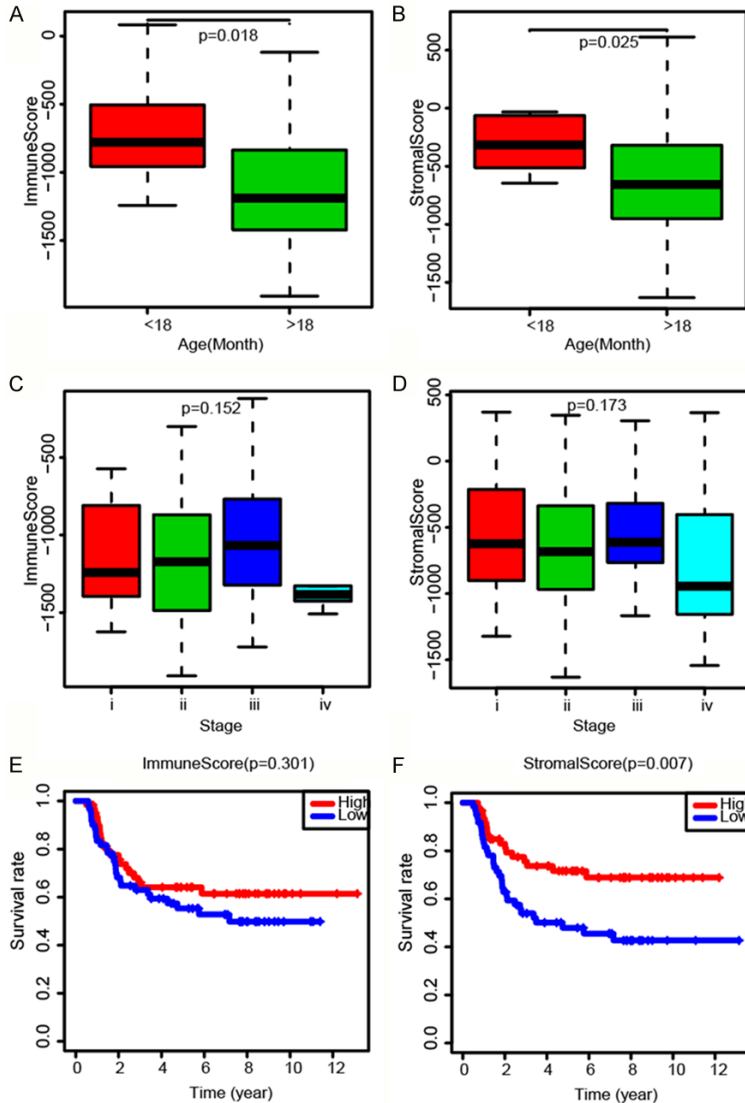


Figure 1. Immune/stromal scores are associated with patients' age, stage and overall survival. A, B. Taking 18 months old as threshold, box-plot shows that there is significant association between age of patients and the level of immune scores ($P=0.018$) and stromal scores ($P=0.025$). C, D. Box-plot shows that there is no significant association between tumor stage and the immune scores ($P=0.152$) and stromal scores ($P=0.173$). E, F. The analysis of patients' overall survival (OS) based on immune scores ($P=0.301$) and stromal scores ($P=0.007$) was shown by Kaplan-Meier survival curve.

terion for both GO and KEGG enrichment analysis.

Construction of the PPI network

The direct and indirect correlations between DEGs was assessed from Search Tool for the Retrieval of Interacting Genes/Proteins (STRING; Version 11.0; <http://string-db.org/>) database [21]. The protein-protein interaction (PPI) network was reconstructed via Cytoscape soft-

ware (Version 3.6.1) [22]. Functionally related clusters were further identified from the PPI network with the Molecular Complex Detection algorithm (MCODE; Version: 1.4.2) in Cytoscape, based on topology to locate densely connected regions.

Results

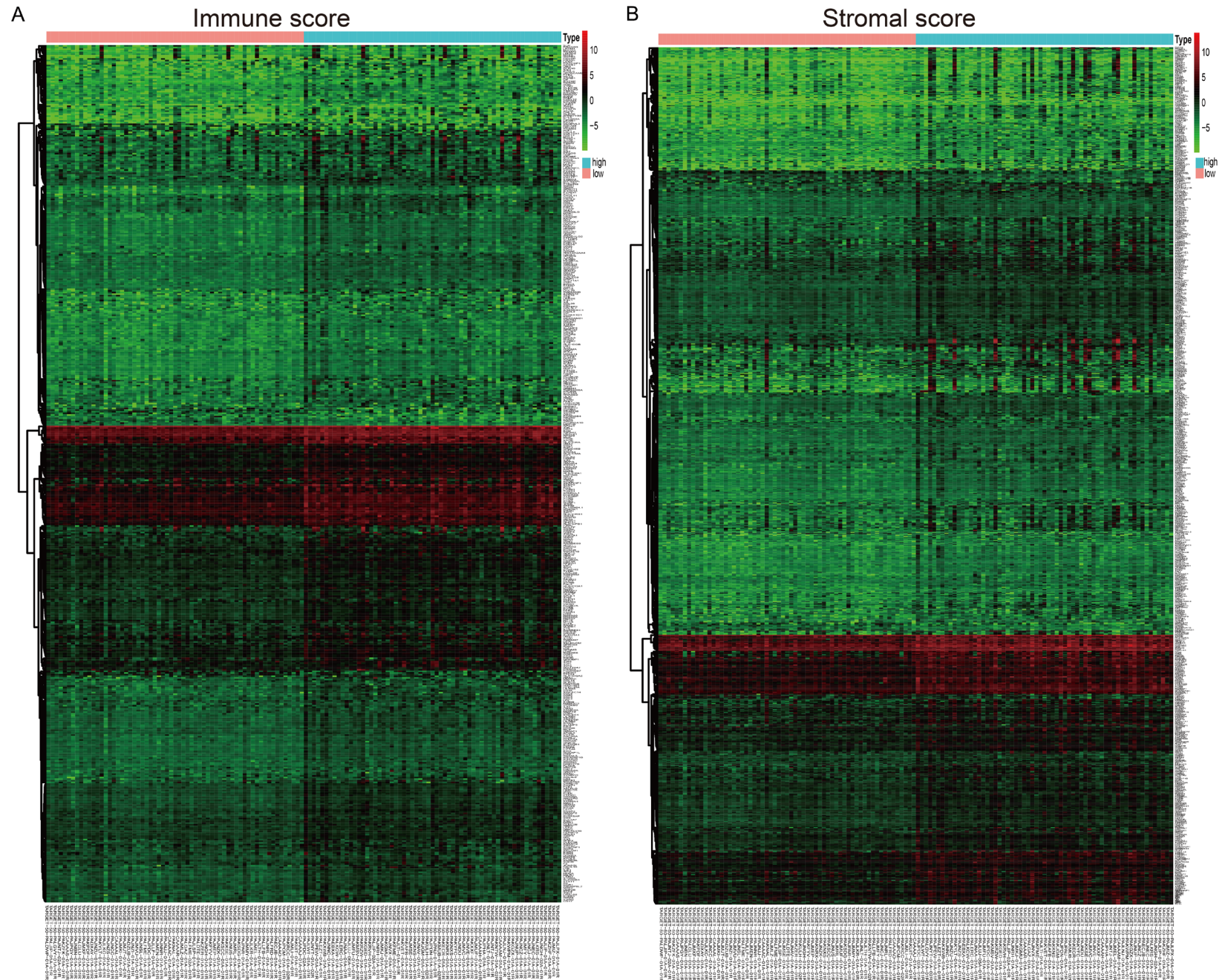
Association of stromal or immune scores with Wilms' tumor prognosis

In this study, the gene expression profile and clinical characteristics of 121 Wilms tumor patients obtained from the TARGET were collected for consequent analysis. The 121 patients in this study ranger between 0-15 years old, with 53 males (43.80%) and 58 (47.93%) females. According to the ESTIMATE algorithm, stromal scores were distributed between 1630.780 and 881.678, and immune scores ranging from -1908.230 to 1035.577.

Taking the median immune/stromal score as the cutoff value, the patients were divided into two groups. As the Wilms tumor is one of the most frequent extra-cranial solid tumors in early childhood, we divided the 121 patients into a younger group (≤ 18 months, $n=7$) and an elder group (>18 months old, $n=114$). As shown

in **Figure 1A** and **1B**, the distribution of immune scores ($P=0.018$) and stromal scores ($P=0.025$) vary across different ages. Compared to elder children, younger children (≤ 18 months old) were with higher immune/stromal scores, which suggested more immune cell infiltration in the tumor. However, no significant associations were observed in other stratified analyses such as tumor stage (**Figure 1C, 1D**). Then, we attempt to explore the potential correlation between prognosis and immune/stromal scor-

Prognostic microenvironment related gene mining in a Wilms tumor



Prognostic microenvironment related gene mining in a Wilms tumor

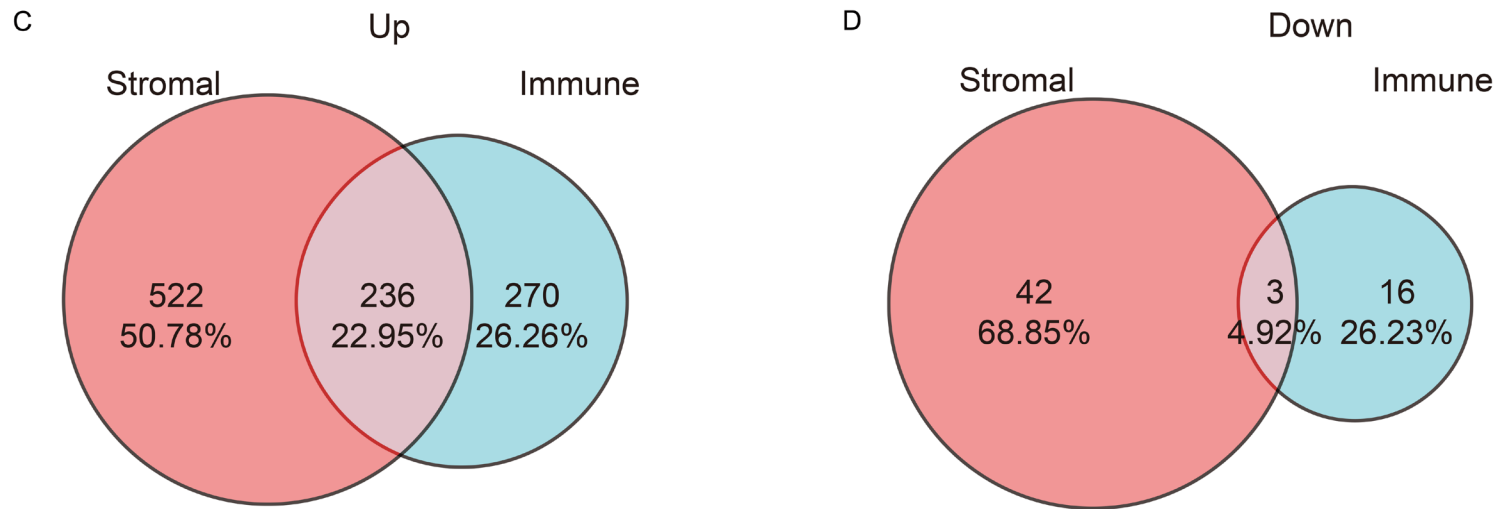


Figure 2. Comparison of gene expression profile with immune scores and stromal scores in Wilms tumors. Wilms tumor patients were divided into two groups based on their immune scores or stromal score. Heatmaps of the DEGs of immune scores (A) or stromal scores (B) of high score group vs. low score group. (FDR<0.05, $\log_2 |FC| > 1$) were drawn. Genes with higher expression are shown in red, lower expression are shown in green, genes with same expression level are in black. Venn diagrams showing the number of aberrantly upregulated (C) or downregulated (D) TME-related DEGs in stromal and immune score groups. DEGs, differentially expressed genes; TME, tumor microenvironment.

Prognostic microenvironment related gene mining in a Wilms tumor

Table 1. The 236 upregulated and 3 downregulated intersect genes

Genes	Regulation
CBR3, LRRC2, SLN, SAMD4A, CXorf21, CD2, MS4A4A, AGT, SFRP2, GAPT, RARRES1, APOD, ALDH1A1, EVI2A, HOPX, SDS, S100A8, ARHGAP15, CYTH4, DPEP2, FOS, SERPINF1, SECTM1, SYNPO2, GPR183, ADRB2, IL2RG, CXCL6, CEBPD, CCR5, RNASE6, PDCD1LG2, TMEM52B, ABI3BP, CSF1R, SHH, IL34, GOS2, HGF, TFEC, TNNI2, FCER1A, MSR1, GIMAP1, BATF, IL6, C1S, MILR1, ADAM12, FGL2, OTOR, VSIG4, GSDMA, CCL2, FIBIN, RNASE2, CFHR1, PTGS2, SRGN, TNNC1, TRIM72, ITIH5, TREM2, SLAMF8, HRCT1, GPR65, ATP6V1G3, TMEM47, MYL4, CD180, PLD4, CCL8, CLRN3, RNASE1, C3, SPP1, ZFP36, KCNJ1, SNX20, SPARCL1, SIGLEC1, FPR3, P2RY13, IL32, CD79B, CD68, APOC1, MGP, HLA-DRA, MNDA, PROCR, KLF5, ANK1, GNA15, EGR2, EVI2B, LGALS1, PTPRC, PTGFR, CSTA, JAML, IL17B, MYF5, CCL26, MARCO, LRRC25, DKK2, GBP5, TRIM22, CLEC3B, CARD16, ITM2A, LY86, CD3G, S1PR4, TNNT2, MPEG1, CLEC2B, PRDM8, LAPTM5, WIF1, KLF2, CASP1, IGF1, LMOD3, PLA2G2A, DCN, BDKRB1, LYZ, CCL11, CD53, CH25H, ATP8B4, MYL3, FCGR1A, LYVE1, FCGR2B, C15orf48, C1QC, SLAMF6, CRYAB, IFIT1, TYROBP, FGF7, TMIGD3, CYR61, CHL1, TIMP4, NCF4, MS4A6A, CD163, SLC22A3, CD84, GPNMB, RGS18, MS4A7, CXCL2, C1QB, FAM124B, GIMAP2, ALDH3B1, SAMSN1, MZB1, PLEK, AQP1, LRTM1, GREM1, RETN, AQP9, IFIT3, MMP19, HSPB3, LAIR1, LGALS3, C1QTNF1, APBB1IP, CD14, FABP4, RAMP1, C4B, RGS1, LY96, AOA, CD300LF, CCR1, C3AR1, MYOZ2, BMX, CLEC10A, CFH, MS4A14, TRIM55, SLC1A3, FABP3, TNNT3, GADD45B, P2RY12, HSD11B1, CXCL10, FDCSP, HES5, BIRC3, THBS1, LRRN4CL, CLDN8, TIMD4, MYLPF, STX11, TLR7, CCL14, CCR7, C1QA, ADAMDEC1, SRPX2, JCHAIN, PTHLH, AIF1, IL10RA, OSM, IL10, FOLR2, CTSS, CEACAM21, XAF1, VSTM2L, HMOX1, SAMD9L, IL1RN, CLEC7A, PARVG, IL33, FPR1, CXCL3, SGK1, EPYC, GPIHBP1	up
TMC2, AMHR2, KCNB2	down

es. Stromal score was significantly positively associated with overall survival of patients (**Figure 1F**, $P=0.007$), while the immune score showed no significant correlation with patients' overall survival (**Figure 1E**, $P=0.301$), indicating that the stromal score may be a positive factor in patient prognosis.

Identification of the DEGs and TME-related DEGs

In the present study, immune related genes were selected by comparing high and low immune/stromal score patients. In high immune-score patients, 506 genes were up-regulated and 19 genes were down-regulated. Similarly, there were 758 up-regulated genes and 45 downregulated genes in the high stromal-score group.

Heatmaps based on these differentially expressed mRNAs were shown in **Figure 2A** and **2B**. Base on the differentially expressed RNAs, the patients with high stromal or immune scores could be clearly distinguished from the patients with low stromal or immune scores. The number of intersection genes which were aberrantly up-regulated or down-regulated in both high-stromal and high-immune score groups was shown by venn diagrams (**Figure 2C** and **2D**) and detected as TME-related DEGs

(236 upregulated genes and 3 downregulated genes, **Table 1**).

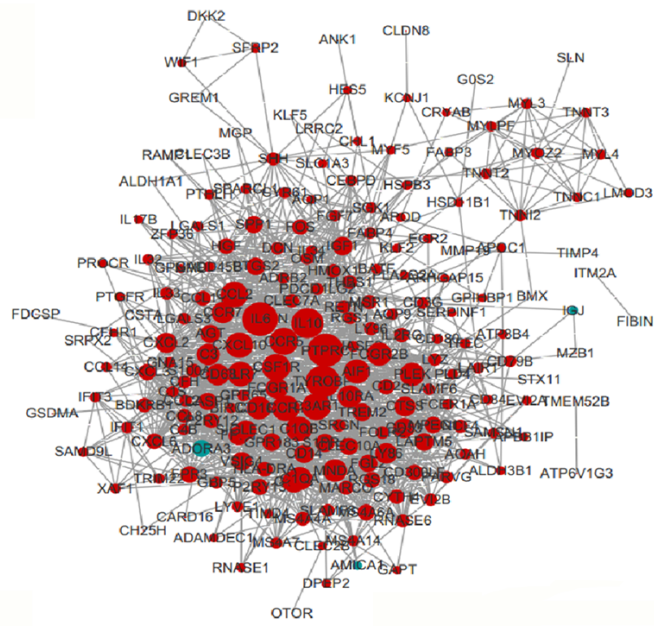
The functional analysis of TME-related DEGs

To better understand the interplay among the identified TME-related DEGs, the protein-protein interaction (PPI) network was obtained by STRING (minimum required interaction score: 0.4). After excluding the proteins with no protein-protein interaction, a PPI network with 205 nodes and 1,697 edges was reconstructed by Cytoscape (**Figure 3A**). The degree distribution of the nodes in this PPI network was analyzed and each node had a relatively high degree, with the average degree of 15.556. The TME-related DEGs with top 30 degree (the interaction number of a protein >34) were shown in **Figure 3B**. To outline the potential function of the TME-related DEGs and hub genes, functional enrichment analysis was performed with "ClusterProfiler". With the 239 TME-related DEGs, 625 Gene Ontology (GO) terms and 26 KEGG pathways were indicated (**Figure 3C, 3D**).

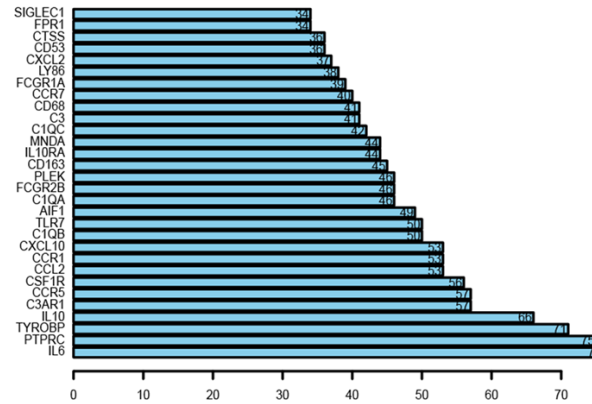
Two clusters, with 25 nodes 194 edges (**Figure 3E**), or 24 nodes 170 edges (**Figure 3F**), were selected by Molecular Complex Detection (MCODE) based on their topology to locate densely connected regions. In cluster 1 (**Figure 3E**), 25 nodes and 194 edges were formed in

Prognostic microenvironment related gene mining in a Wilms tumor

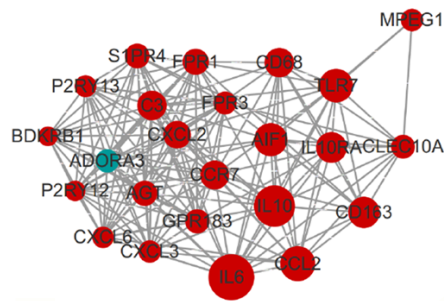
A



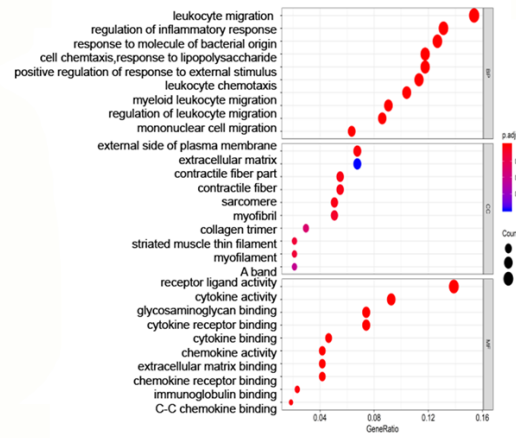
B



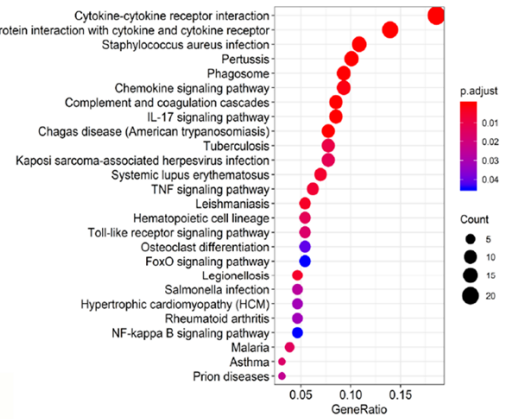
E



C



D



Prognostic microenvironment related gene mining in a Wilms tumor

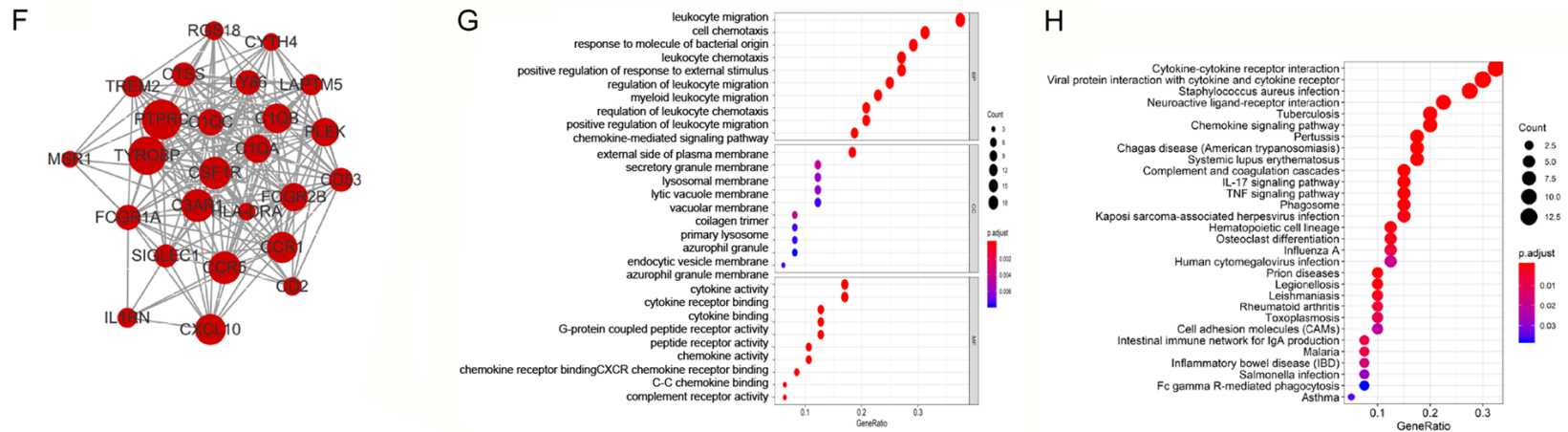


Figure 3. The functional analysis of TME-related DEGs and hub genes. A. The PPI network (protein-protein interaction network) in TME-related DEGs. B. The degree distribution of PPI network of the top 30 TME-related DEGs. C. The top 10 predominant BP, CC and MF terms enriched by these aberrantly expressed TME-related DEGs. D. The top 30 predominant KEGG pathways enriched by these aberrantly expressed TME-related DEGs. E, F. Top two modules in the PPI networks. G. The top 10 predominant BP, CC and MF terms enriched by the hub genes. H. The top 30 predominant KEGG pathways enriched by the hub genes. The color of node reflects the upregulation (red) of downregulation (blue) of TME-related DEGs, and the size of the node indicates the number of proteins interacting with the designated protein. PPI network, protein-protein interaction network; TME, tumor microenvironment; MCODE, Molecular Complex Detection; MF, molecular function; BP, biological process; CC, cellular component; KEGG, Kyoto Encyclopedia of Genes and Genomes.

Prognostic microenvironment related gene mining in a Wilms tumor

Table 2. The hub genes involve in the top two clusters

Hub genes in cluster 1	FCGR2B, SIGLEC1, CYTH4, C1QC, C1QB, IL1RN, PTPRC, MSR1, LY86, LAPTM5, C1QA, FCGR1A, PLEK, RGS18, CSF1R, TREM2, CCR1, TYROBP, HLA-DRA, CXCL10, CCR5, CD2, C3AR1, CD53, CTSS
Hub genes in cluster 2	AIF1, CXCL2, IL6, CCL2, CXCL6, AGT, FPR1, CXCL3, BDKRB1, ADORA3, CLEC10A, P2RY12, CD68, GPR183, C3, MPEP1, FPR3, P2RY13, CCR7, IL10, S1PR4, IL10RA, CD163, TLR7

the network. Among them PTPRC, TYROBP, CCR5, C3AR1, CSF1R, CCR1, CXCL10, C1QB, PLEK and C1QA were remarkable for having many connections with other DEGs. In cluster 2 (Figure 3F), there were 24 nodes and 170 edges, IL6, IL10, CCL2, TLR7, AIF1, CD163, IL10RA, C3, CD68 and CCR7 had higher connectivity degree values. Among the top 30 DEGs, some genes such as IL-6, PTPRC, TYROBP, IL-10, CCR5, CSF1R, CCL2 and CCR1 were core genes in the top two clusters and they were significantly associated with migration and function of immune cells in the tumor microenvironment.

The DEGs involved in the top two clusters were taken as hub genes (shown in Table 2). Among them, PTPRC, also named CD45, is present on all differentiated hematopoietic cells (except erythrocytes and plasma cells) in various isoforms [23]. TYROBP which is mainly expressed on peripheral monocyte-macrophage system [24] is regarded as a key component in macrophage activation signals and inhibitory signals [25, 26]. CXCL10 was reported to recruit monocyte-derived macrophages in to the kidney in puromycin aminonucleoside nephrosis [27]. What's more, CD163 and CD68 were biomarkers of macrophages, the cytokines such as IL6, IL10 and chemokines such as CCL2, CXCL10 were associated with the recruitment and function of macrophages. Our data indicated that the monocyte-macrophage system may play a key role in Wilms tumors. The functional analysis of the 49 hub genes showed that 424 Gene Ontology (GO) terms and 37 KEGG pathways were indicated (Figure 3G, 3H). Overall, the results suggested that most of these genes were relative to the tumor microenvironment.

Survival analysis of TME-related DEGs

We analyzed the relationships between the expression of 239 TME-related DEGs and the overall survival based on the clinical information. Then, $P < 0.05$ was selected as the thresh-

old to obtain 11 prognosis-related genes. The high expression of these 11 genes, including GSDMA, TRIM55, SPARCL1, EPYC, LRRC2, LAPTM5, PTGFR, APOD, IGF1, CEBPD and SF-RP2, was associated with favorable patient prognosis and they may be studied in our further research (Figure 4).

Discussion

Wilms tumors (~85% of all cases in TARGET Kidney Tumor projects) is one of the most common categories in pediatric kidney tumors that may spread to the lungs, liver, bone, brain, or nearby lymph nodes in later stages [2], which may seriously affect the survival and prognosis of patients. To some extent the current treatment of Wilms tumors such as surgery, chemotherapy, and radiation therapy are successful; the cure rate and survival period of Wilms tumors have increased to approximately 90% [3]. However, young children are at a high risk for the irreversible adverse side effects and there are still 10% of patients with Wilms tumors who die due to recurrence. Thus, the occurrence and development of Wilms tumors needs positive attention worldwide. With the development of sequencing technology, more and more somatic and germline information were revealed to be responsible for Wilms tumors [6]. However, effective prognostic biomarkers that could serve to guide Wilms tumor therapy and prognosis are still lacking.

The tumor microenvironment is determined by many factors including genetic factors. However, there have been few previous studies of the tumor microenvironment of Wilms tumors. In the current study, we explored the tumor microenvironment based on the TARGET database, with the largest collection of Wilms tumor samples in a public database and focused on the Wilms tumor immune microenvironment-related gene characteristics. We found that immune and stromal scores were inversely correlated with patients' age but positively

Prognostic microenvironment related gene mining in a Wilms tumor

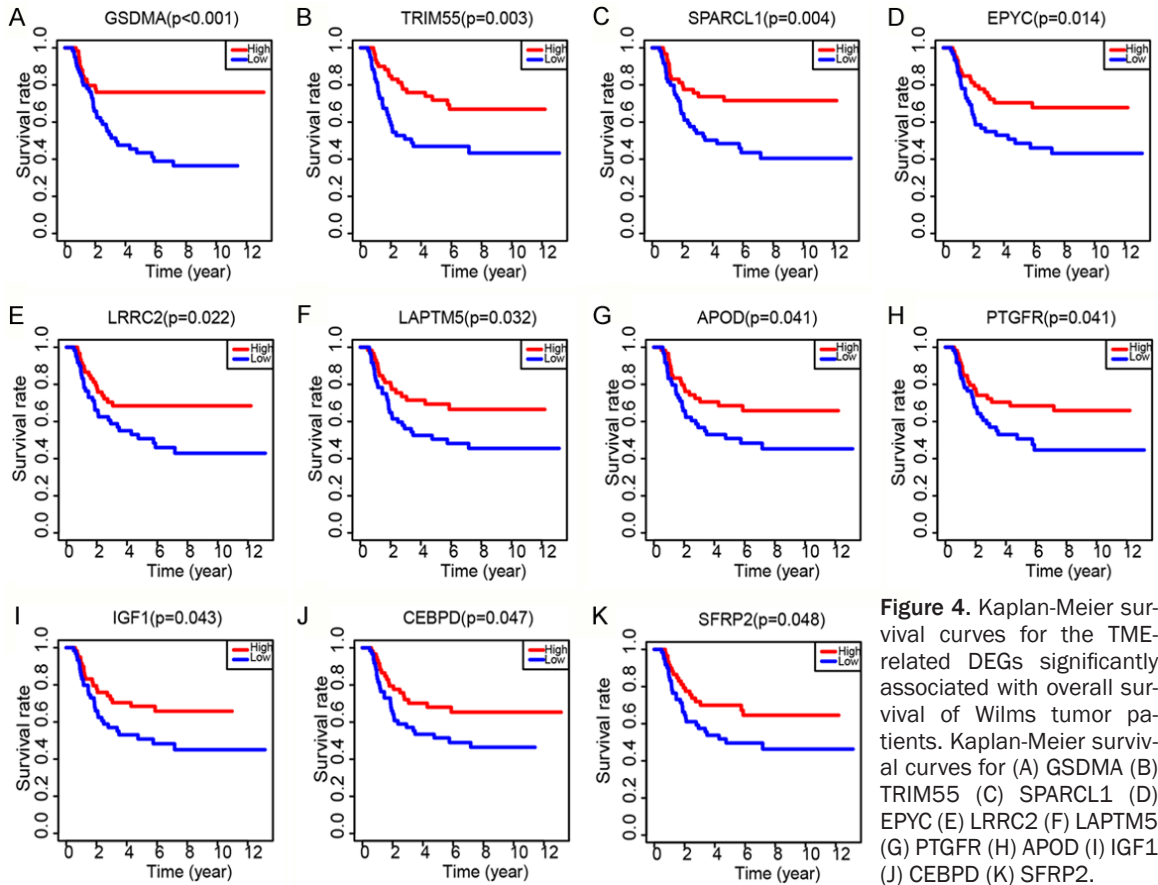


Figure 4. Kaplan-Meier survival curves for the TME-related DEGs significantly associated with overall survival of Wilms tumor patients. Kaplan-Meier survival curves for (A) GSDMA (B) TRIM55 (C) SPARCL1 (D) EPYC (E) LRRC2 (F) LAPT5 (G) PTGFR (H) APOD (I) IGF1 (J) CEBPD (K) SFRP2.

correlated overall survival. In particular, by comparing gene expression in 121 Wilms tumor patients with high or low immune scores, differentially expressed genes (DEGs) were yielded. A total of 239 TME-related DEGs were extracted which were aberrantly up-regulated or downregulated in both high-stromal and high-immune score patients.

Tumor associated macrophages with M2 phenotype were reported to affect pathological outcome, tumor grade, angiogenesis and invasiveness in many tumors [28, 29]. In Wilms tumors, infiltration of macrophages was defined as a major nosologic difference with adult tumors [30]. To further identify functional TME-related DEGs, the PPI modules were constructed. Nodes with a high connectivity degree in the modules, including IL-6, IL-10, CSF1R, CCL2 and CXCL10, were related to proliferation, apoptosis and function of immune cells especially monocyte-macrophage system [31-33]. In line with these results, the GO and KEGG analysis showed that many of the TME-related DEGs and hub genes were involved in regulation of

inflammatory response or migration and chemotaxis of immune cells especially macrophages (GO:0050900 leukocyte migration, GO:0050727 regulation of inflammatory response, GO:0060326 cell chemotaxis, GO:0005-126 cytokine receptor binding, GO:0019955 cytokine binding, hsa04060 Cytokine-cytokine receptor interaction, hsa04061 Viral protein interaction with cytokine and cytokine receptor). Then an overall survival analysis of all TME-related DEGs was performed. A total of 11 genes were detected to be associated with outcomes of patients. However, all these 11 genes seemed to be less perfect prognostic biomarkers with ROC analysis (AUC between 0.6-0.7). We believe that this may be due to the small sample size (only 120 samples) enrolled in this study. Wilms tumor is the most common kidney cancer in children but relatively rare in absolute numbers (1 in 10,000 children). Although TARGET database had the largest collection of Wilms tumors in a public database, there were only 120 samples enrolled in our study. We believe that a perfect prognostic marker among

Prognostic microenvironment related gene mining in a Wilms tumor

these 11 genes would be identified if we have a larger sample size.

In summary, to our knowledge, despite the limited sample size, the present study is the first to apply bioinformatics analysis to Wilms tumors and has provided more data for decoding the complicated microenvironment. This study will help to mine new and potential immune associated biomarkers and therapeutic targets for the diagnosis and prognosis prediction of Wilms tumors.

Acknowledgements

Foundation of Development and Related Diseases of Women and Children Key Laboratory of Sichuan Province, grant number No. 2022-003; Foundation of Basic research project of Nursing Department, grant number NO. HLBKJ202126, Foundation of Science and Technology Planning Project of Sichuan province 2021YJ0011.

Disclosure of conflict of interest

None.

Address correspondence to: Dr. Tao Yi, West China Second Hospital, Sichuan University, No. 17, Section 3, Renmin Road South, Chengdu 610041, Sichuan, China. Tel: +86-28-85502822; Fax: +86-28-8550-2822; E-mail: 44128579@qq.com

References

- [1] Breslow N, Olshan A, Beckwith JB and Green DM. Epidemiology of Wilms tumor. *Med Pediatr Oncol* 1993; 21: 172-181.
- [2] Vujančić GM and Sandstedt B. The pathology of Wilms' tumour (nephroblastoma): the international society of paediatric oncology approach. *J Clin Pathol* 2010; 63: 102-109.
- [3] Dome JS, Graf N, Geller JI, Fernandez CV, Mullen EA, Spreafico F, Van den Heuvel-Eibrink M and Pritchard-Jones K. Advances in Wilms tumor treatment and biology: progress through international collaboration. *J Clin Oncol* 2015; 33: 2999.
- [4] He J, Guo X, Sun L, Wang K and Yao H. Networks analysis of genes and microRNAs in human Wilms' tumors. *Oncol Lett* 2016; 12: 3579-3585.
- [5] Yan Z, Meng Q, Yang J, Zhang J, Zhao W, Guo F, Song D, Zhan Y, Fan D and Zhou R. Identification of proteins associated with pediatric bilateral Wilms tumor. *Oncol Lett* 2016; 12: 5075-5079.
- [6] Zhu J, Jia W, Wu C, Fu W, Xia H, Liu G and He J. Base excision repair gene polymorphisms and Wilms tumor susceptibility. *EBioMedicine* 2018; 33: 88-93.
- [7] Maturu P, Overwijk WW, Hicks J, Ekmekcioglu S, Grimm EA and Huff V. Characterization of the inflammatory microenvironment and identification of potential therapeutic targets in wilms tumors. *Transl Oncol* 2014; 7: 484-492.
- [8] Little SE, Hanks SP, King-Underwood L, Jones C, Rapley EA, Rahman N and Pritchard-Jones K. Frequency and heritability of WT1 mutations in nonsyndromic Wilms' tumor patients: a UK children's cancer study group study. *J Clin Oncol* 2004; 22: 4140-4146.
- [9] Scott RH, Douglas J, Baskcomb L, Huxter N, Barker K, Hanks S, Craft A, Gerrard M, Kohler JA and Levitt GA. Constitutional 11p15 abnormalities, including heritable imprinting center mutations, cause nonsyndromic Wilms tumor. *Nat Genet* 2008; 40: 1329.
- [10] Andrade R, Cardoso L, Ferman S, Faria P, Seuanez HN, Achatz M and Vargas F. Association of TP53 polymorphisms on the risk of Wilms tumor. *Pediatr Blood Cancer* 2014; 61: 436-441.
- [11] Binnewies M, Roberts EW, Kersten K, Chan V, Fearon DF, Merad M, Coussens LM, Gabriilovich DI, Ostrand-Rosenberg S and Hedrick CC. Understanding the tumor immune microenvironment (TIME) for effective therapy. *Nat Med* 2018; 24: 541-550.
- [12] Quail DF and Joyce JA. Microenvironmental regulation of tumor progression and metastasis. *Nat Med* 2013; 19: 1423-1437.
- [13] Overchuk M and Zheng G. Overcoming obstacles in the tumor microenvironment: recent advancements in nanoparticle delivery for cancer theranostics. *Biomaterials* 2018; 156: 217-237.
- [14] Karth J, Ferrer FA, Perlman E, Hanrahan C, Simmons JW, Gearhart JP and Rodriguez R. Coexpression of hypoxia-inducible factor 1-alpha and vascular endothelial growth factor in Wilms' tumor. *J Pediatr Surg* 2000; 35: 1749-1753.
- [15] Yoshihara K, Shahmoradgoli M, Martínez E, Vegesna R, Kim H, Torres-Garcia W, Treviño V, Shen H, Laird PW and Levine DA. Inferring tumor purity and stromal and immune cell admixture from expression data. *Nat Commun* 2013; 4: 2612.
- [16] Shah N, Wang P, Wongvipat J, Karthaus WR, Abida W, Armenia J, Rockowitz S, Drier Y, Bernstein BE and Long HW. Regulation of the glucocorticoid receptor via a BET-dependent enhancer drives antiandrogen resistance in prostate cancer. *Elife* 2017; 6: e27861.
- [17] Priedigkeit N, Watters RJ, Lucas PC, Basudan A, Bhargava R, Horne W, Kolls JK, Fang Z, Rosenzweig MQ and Brufsky AM. Exome-capture RNA sequencing of decade-old breast

Prognostic microenvironment related gene mining in a Wilms tumor

- cancers and matched decalcified bone metastases. *JCI insight* 2017; 2: e95703.
- [18] Di Jia SL, Li D, Xue H, Yang D and Liu Y. Mining TCGA database for genes of prognostic value in glioblastoma microenvironment. *Aging (Albany NY)* 2018; 10: 592.
- [19] Alonso MH, Aussó S, Lopez-Doriga A, Cordero D, Guinó E, Solé X, Barenys M, de Oca J, Capella G and Salazar R. Comprehensive analysis of copy number aberrations in microsatellite stable colon cancer in view of stromal component. *Br J Cancer* 2017; 117: 421.
- [20] Yu G, Wang LG, Han Y and He QY. clusterProfiler: an R package for comparing biological themes among gene clusters. *OMICS* 2012; 16: 284-287.
- [21] Szklarczyk D, Gable AL, Lyon D, Junge A, Wyder S, Huerta-Cepas J, Simonovic M, Doncheva NT, Morris JH and Bork P. STRING v11: protein-protein association networks with increased coverage, supporting functional discovery in genome-wide experimental datasets. *Nucleic Acids Res* 2018; 47: D607-D613.
- [22] Kohl M, Wiese S and Warscheid B. Cytoscape: software for visualization and analysis of biological networks. *Data mining in proteomics*. Springer; 2011. pp. 291-303.
- [23] Holmes N. CD45: all is not yet crystal clear. *Immunology* 2006; 117: 145-155.
- [24] Hamerman JA, Ni M, Killebrew JR, Chu CL and Lowell CA. The expanding roles of ITAM adaptors FcRγ and DAP12 in myeloid cells. *Immunol Rev* 2009; 232: 42-58.
- [25] Turnbull IR and Colonna M. Activating and inhibitory functions of DAP12. *Nat Rev Immunol* 2007; 7: 155-61.
- [26] Peng Q, Long CL, Malhotra S and Humphrey MB. A physical interaction between the adaptor proteins DOK3 and DAP12 is required to inhibit lipopolysaccharide signaling in macrophages. *Sci Signal* 2013; 6: ra72.
- [27] Petrovic-Djergovic D, Popovic M, Chittiprol S, Cortado H, Ransom RF and Partida-Sánchez S. CXCL10 induces the recruitment of monocyte-derived macrophages into kidney, which aggravate puromycin aminonucleoside nephrosis. *Clin Exp Immunol* 2015; 180: 305-315.
- [28] Takeuchi H, Tanaka M, Tanaka A, Tsunemi A and Yamamoto H. Predominance of M2polarized macrophages in bladder cancer affects angiogenesis, tumor grade and invasiveness. *Oncol Lett* 2016; 11: 3403-3408.
- [29] Li Z, Xu Z, Huang Y, Zhao R, Cui Y, Zhou Y and Wu X. The predictive value and the correlation of peripheral absolute monocyte count, tumor-associated macrophage and microvessel density in patients with colon cancer. *Medicine (Baltimore)* 2018; 97: e10759.
- [30] Vakkila J, Jaffe R, Michelow M and Lotze MT. Pediatric cancers are infiltrated predominantly by macrophages and contain a paucity of dendritic cells: a major nosologic difference with adult tumors. *Clin Cancer Res* 2006; 12: 2049-2054.
- [31] Pyonteck SM, Akkari L, Schuhmacher AJ, Bowman RL, Sevenich L, Quail DF, Olson OC, Quick ML, Huse JT and Teijeiro V. CSF-1R inhibition alters macrophage polarization and blocks glioma progression. *Nat Med* 2013; 19: 1264-72.
- [32] Lin EY, Nguyen AV, Russell RG and Pollard JW. Colony-stimulating factor 1 promotes progression of mammary tumors to malignancy. *J Exp Med* 2001; 193: 727-740.
- [33] Qian BZ, Li J, Zhang H, Kitamura T, Zhang J, Campion LR, Kaiser EA, Snyder LA and Pollard JW. CCL2 recruits inflammatory monocytes to facilitate breast-tumour metastasis. *Nature* 2011; 475: 222-U129.